Redox Biology 80 (2025) 103521

Contents lists available at ScienceDirect

Redox Biology

journal homepage: www.elsevier.com/locate/redox

ROS anchor PAMPs-mediated extracellular HMGB1 self-association and its dimerization enhances pro-inflammatory signaling

Man Sup Kwak [a,b,**], Myeonggil Han [a,c], Yong Joon Lee [a], Seoyeon Choi [a,c], Jeonghwa Kim [a,c], In Ho Park [b,d], Jeon-Soo Shin [a,b,c,*]

[a] Department of Microbiology, Yonsei University College of Medicine, Seoul, 03722, South Korea
[b] Institute for Immunology and Immunological Diseases, Yonsei University College of Medicine, Seoul, 03722, South Korea
[c] Brain Korea 21 FOUR Project for Medical Science, Yonsei University College of Medicine, Seoul, 03722, South Korea
[d] Department of Biomedical Sciences, Yonsei University College of Medicine, Seoul, 03722, South Korea

ARTICLE INFO

Keywords:
HMGB1
Reactive oxygen species
Dimerization
Inflammation

ABSTRACT

Many cellular proteins form homo- or hetero-oligomeric complexes through dimerization, and ligand oligomerization is crucial for inducing receptor oligomerization. Intermolecular disulfide bond formation is critical for protein oligomerization that regulates biological functions. HMGB1 is a nuclear protein that acts as a DAMP when secreted. HMGB1 is redox-sensitive, contains three cysteines: Cys^{23}, Cys^{45}, and Cys^{106}, and its function varies depending on the redox state of the extracellular space. However, the homo-dimerization of extracellular HMGB1 and its immunological significance have not been identified. In this study, we investigated the immunological significance of Cys^{106}-mediated HMGB1 homo-dimerization. In the extracellular environment, LPS and LTA induced HMGB1 self-association leading to H_2O_2 anchoring Cys^{106}–Cys^{106}-mediated HMGB1 intermolecular disulfide bond formation. Despite treatment with H_2O_2, LPS, or LTA, HMGB1 dimerization was blocked in presence of Cys^{106} residue mutation, the ROS scavenger NAC, and the thiol-reducing agent DTT. Inflammatory stimulation induced the secretion of monomeric HMGB1 but not dimeric HMGB1. HMGB1 dimerization was promoted by PAMPs and H_2O_2 in the extracellular environment. Compared to monomeric HMGB1, Cys^{106}–Cys^{106}-linked dimeric HMGB1 significantly enhanced intracellular NF-κB signaling and cytokine production through increased direct binding affinity for TLR2 and TLR4 and effective HMGB1-mediated delivery of PAMPs to their receptors. Therefore, we have demonstrated that dimeric HMGB1 enhances its effect on pro-inflammatory signaling.

1. Introduction

Many proteins function as dimeric homo- or hetero-oligomeric complexes within cells, which often represent their active forms. These complexes enhance the diversity and specificity of cellular signaling by regulating gene expression [1,2], enzyme activity [3–5], and interactions with partner molecules [6,7]. Intermolecular disulfide bond formation is a key mechanism underlying the homo- and/or hetero-oligomerization of proteins.

High mobility group box 1 (HMGB1) is an abundant and ubiquitously expressed nuclear protein, functioning as a DNA chaperone within the nucleus. HMGB1 binds to DNA and participates in DNA replication, recombination, transcription, repair, and genomic stability [8,9]. HMGB1 consists of two homologous, positively charged DNA-binding domains (A- and B-box) and a highly acidic C-tail composed of repeated aspartate and glutamate residues [10]. The A- and B-boxes bind to the minor grooves of DNA without sequence specificity, whereas the C-tail binds to histone proteins, regulating DNA bending [11,12]. Excessive intracellular reactive oxygen species (ROS) induces intracellular HMGB1 homo-dimerization in the nucleus, which increases DNA binding affinity and prevents ROS-mediated DNA damage [13].

HMGB1 also serves as an extracellular signaling molecule [10,14,15], being passively released by necrotic cells and actively secreted by immune cells such as monocytes and macrophages [16–20]. Various posttranslational modifications (PTMs) of HMGB1 enhance its interaction with the nuclear transport receptor chromosome region maintenance 1 (CRM1), leading to its cytoplasmic accumulation [10,21–23].

* Corresponding author. Department of Microbiology, Yonsei University College of Medicine, 50-1 Yonsei-ro Seodaemun-gu, Seoul, 03722, South Korea.
** Corresponding author. Department of Microbiology, Yonsei University College of Medicine, 50-1 Yonsei-ro Seodaemun-gu, Seoul, 03722, South Korea.
E-mail addresses: mskwak@yuhs.ac (M.S. Kwak), jsshin6203@yuhs.ac (J.-S. Shin).

https://doi.org/10.1016/j.redox.2025.103521
Received 16 December 2024; Received in revised form 23 January 2025; Accepted 28 January 2025
Available online 31 January 2025

Abbreviations:

CRM1	Chromosome region maintenance 1
DAMPs	Damage-associated molecular patterns
Di-HMGB1	Dimerized HMGB1 (HMGB1 dimer via Cys^{106} linkage)
Ds-HMGB1	Disulfide HMGB1 (disulfide link between Cys^{23} and Cys^{45})
DTT	Dithiothreitol
ELISA	Enzyme linked immunosorbent assay
GFP	Green fluorescent protein
Grx	Glutaredoxin
HEK	Human embryonic kidney
HMGB1	High mobility group box 1
$(HMGB1)_2$	HMGB1:linker:HMGB1 (two HMGB1 linked by cloning)
IL-1	Interleukin-1
LK	Linker
LPS	Lipopolysaccharide
LTA	Lipoteichoic acid
*s*LTA	LTA from *Staphylococcus aureus*
*b*LTA	LTA from *Bacillus subtilis*
MD2	Myeloid differentiation-2
NAC	*N*-acetylcysteine
PAMP	Pathogen-associated molecular pattern
Prx	Peroxiredoxin
RAGE	Receptor for advanced glycation endproducts
Re-HMGB1	Reduced HMGB1 (reduced residues of Cys^{23} and Cys^{45})
ROS	Reactive oxygen species
SPR	Surface plasmon resonance
S100B	S100 calcium-binding protein B
TLR	Toll-like receptor
Trx	Thioredoxin
TrxR	Thioredoxin reductase
TNF	Tumor necrosis factor
WCL	Whole cell lysate

The autophagy machinery and the formation of multivesicular bodies are crucial for the extracellular secretion of accumulated HMGB1 from the cytoplasm [24]. The released HMGB1 acts as a damage-associated molecular pattern (DAMP) by binding to various receptors, including receptor for advanced glycation endproducts (RAGE), toll-like receptor (TLR)-2, −4, −9, and the type I interleukin-1 (IL-1) receptor, either directly or in complex with selected ligands [25–32]. Receptor oligomerization is an early step in intracellular signaling, accompanied by the recruitment of downstream signaling molecules. TLR2, TLR4, and RAGE are HMGB1 receptors that can be oligomerized by their respective ligands, such as lipoteichoic acid (LTA), lipopolysaccharide (LPS), and S100 calcium-binding protein B (S100B), respectively [33–37]. Ligand oligomerization leads to receptor oligomerization and subsequent downstream signaling. S100B, a RAGE ligand, oligomerization induces high binding affinity for RAGE, resulting in robust activation of cell growth [36,38]. The oligomerized RagA pneumococcal pilus type 1 protein can recognize TLR2 and induce an inflammatory response [39]. Recent studies using surface plasmon resonance (SPR) have reported that HMGB1 can be oligomerized (dimer and tetramer) at physiological ionic strength (150 mM) and pH 7.4 [40,41]. Additionally, HMGB1 oligomerization is sensitive to divalent metal cations such as calcium, magnesium, and zinc [42]. Previously, we identified HMGB1 dimerization in mouse serum after LPS injection under non-reducing Western blot analysis [13]. However, HMGB1 oligomer binding to receptors and modulate their signaling has not been evidenced.

HMGB1 is a redox-sensitive protein that contains the following three cysteine residues: Cys^{23}, Cys^{45}, and Cys^{106}. Peroxiredoxin (Prx) I/II-mediated intramolecular disulfide bond formation between Cys^{23} and Cys^{45} of HMGB1 is required for cytoplasmic translocation and extracellular secretion from the nucleus [23]. Additionally, the formation of the Cys^{23}–Cys^{45} disulfide and free thiol of Cys^{106} are essential for NF-κB stimulation and TNF-α production in macrophages. Mutation of Cys^{106} in HMGB1 abolishes TNF-α stimulating activity, despite the presence of Cys^{23}-Cys^{45} disulfide bond [43,44]. The reduced state of all cysteine residues in HMGB1 allows it to form a complex with CXCL12, which binds to the CXCR4 and induces chemotaxis [45,46]. Thus, the redox status of HMGB1 significantly affects its function and determines its interactions with various receptors.

In this study, we demonstrate that inflammatory stimuli such as LPS from Gram-negative bacteria and LTA from Gram-positive bacteria serve as platforms for HMGB1 self-association by facilitating ROS-mediated Cys^{106}-Cys^{106} intermolecular interactions. The Cys^{106}-mediated dimerized HMGB1 (Di-HMGB1) exhibits higher binding affinity to TLR2 and TLR4 than to monomeric HMGB1. Di-HMGB1 significantly enhances NF-κB signaling and TNF-α production. Our data suggest that Di-HMGB1 could be a novel therapeutic target for improving immune disorders.

2. Materials and methods

2.1. Cell culture and transfection

Human embryonic kidney 293T (HEK293T), HEK293-hTLR4A/MD2/CD14 (Invivogen, 293-htlr4md2cd14), RAW264.7, and J774A.1 cells were cultured in Dulbecco's modified Eagle's medium (DMEM) supplemented with 10% FBS (Corning Cellgro, 35-015-CV), 100 U/mL penicillin, 100 μg/mL streptomycin, and 2 mM L-glutamine, at 37°C under 5% CO_2. Additionally, HEK293-hTLR4A/MD2/CD14 cells were cultured in the above-mentioned culture medium supplemented with 100 μg/mL Normocin™ (InvivoGen) and the selected antibiotics, 10 μg/mL blasticidin and 50 μg/mL hygromycin B. For transfection, the cells were seeded for 24 h, grown to 80–90% confluency, and transfected using FuGeneHD reagent (Promega Corporation, E2311).

2.2. Plasmid construction

To determine the function of HMGB1 dimerization, Myc-, EGFP-tagged HMGB1, HMGB1:linker (LK):HMGB1 [$(HMGB1)_2$], and the C106A mutant of HMGB1 ($HMGB1^{C106A}$) were cloned using the pCMV-Myc (Clontech) vector for overexpression studies. Six His-tagged plasmids were generated using the pRSET.B (Invitrogen) vector for recombinant protein production. For $(HMGB1)_2$, two repeats of HMGB1 with the same orientation were cloned via a LK, a Ser-$(Gly)_4$-Ser for flexibility. The N-terminal half of GFP [amino acids 1–155 (GFP^N)] and the C-terminal half of GFP [amino acids 156–238 (GFP^C)]-tagged HMGB1 plasmids had been cloned previously [13]. GFP^N and GFP^C were linked via the same linker fused at the 5′- or 3′-end of HMGB1 (GFP^N-HMGB1, GFP^C-HMGB1, or HMGB1-GFP^C) and were subcloned into the pCMV-Myc vector to study the binding orientation of two HMGB1 molecules.

2.3. Purification of recombinant HMGB1

The HMGB1, $(HMGB1)_2$, and $HMGB1^{C106A}$ mutant proteins were purified as previously described [16,22]. They were expressed in SoluBL21 competent *E. coli,* lysed by sonication, and sequentially processed for purification via Ni^{2+}-NTA, heparin, and gel-filtration column chromatography. The intramolecular Cys^{23}-Cys^{45} disulfide form of HMGB1 (Ds-HMGB1) was produced and purified using cell lysis buffer without dithiothreitol (DTT) and elution buffer. In the HMGB1 purification process, endotoxin was removed by phase separation using 1% v/v

Triton X-114 [47] and confirmed as less than 1 EU/μg protein using the *Limulus* amebocyte lysate assay (Lonza Bioscience, 50–650U).

2.4. HMGB1 dimerization

To determine the binding affinity to TLRs and activation of NF-κB signaling, Di-HMGB1 was prepared by incubating HMGB1 protein in PBS containing 10 μM $CuCl_2$ with 50 μM H_2O_2 at 37°C for 18 h, or 50 μM H_2O_2 with 10 ng/mL LPS or LTA for 1 h and 17 h, respectively. To observe the facilitation of HMGB1 dimerization *in vitro*, 100 ng/μL HMGB1 and $HMGB1^{C106A}$ proteins were incubated at 37°C in normal mouse serum with LPS from *Escherichia coli* 0111:B4 (Sigma-Aldrich, L5293) and lipoteichoic acids (LTAs) from *Staphylococcus aureus* (*s*LTA) (Invivogen, tlrl-pslta) and *Bacillus subtilis* (*b*LTA) (Sigma, L3265). Various concentrations of H_2O_2, 5 mM DTT, and 50 μM N-acetylcysteine (NAC) were used for oxidation or reduction. Polymyxin B (30 μg/mL) was used for LPS neutralization. Test samples were 20-fold diluted and 100 ng of protein was loaded for Western blot analysis under non-denaturing conditions without β-mercaptoethanol.

2.5. Immunoprecipitation and immunoblotting

To identify the binding of HMGB1 to TLR4/MD2 (R&D Systems, 3146-TM/CF), the proteins HMGB1, Di-HMGB1, and $HMGB1^{C106A}$ were incubated with a mixture of TLR4/MD2 in PBS at 37°C for 2 h. The complex mixtures were then added to mouse anti-TLR4 antibody (Cayman, 13589), which had been conjugated to Dynabead protein G (Biorad, 1614023), at incubated at 4°C for 18 h. The beads were washed three times with PBST and then mixed with protein sample buffer. After heating at 95°C for 10 min, the proteins were separated by SDS-PAGE, and immunoblotted with rabbit anti-HMGB1 (Abcam, ab18256), rabbit anti-MD2 (Abcam, ab24182), and rabbit anti-TLR4 (Sigma-Aldrich, SAB5700648) antibodies.

HEK293T and HEK293-hTLR4A/MD2/CD14 cells were transfected with each plasmid in six-well plates using FuGene HD for 24 h. The cells were then lysed with 1 × radioimmunoprecipitation assay buffer (RIPA) buffer (GenDePOT, R4100) containing 150 mM NaCl, 1% Triton X-100, 1% deoxycholic acid sodium salt, 0.1% SDS, 50 mM Tri-HCl (pH 7.5), 2 mM EDTA, and a protease inhibitor cocktail (GenDEPOT, HY-K0010) along with a phosphatase inhibitor cocktail (Thermo Scientific™, 78420). Whole-cell lysates (WCLs) were centrifuged at 20,000×*g* at 4°C for 10 min. A protein sample buffer containing 100 mM Tris-HCl (pH 6.8), 2% SDS, 25% glycerol, and 0.1% bromophenol blue was added to WCLs with or without 5% β-mercaptoethanol, followed by heating at 95°C for 10 min. The proteins were separated by SDS-PAGE and transferred to a nitrocellulose membrane (GE Healthcare, 10600001). After blocking with Tris-buffered saline (TBS) with 5% skim milk (w/v) for 1 h, the membranes were incubated with rabbit anti-HMGB1, mouse anti-Myc (Invitrogen, 13–2500), rabbit anti-MD2, rabbit anti-phospho–NF–κB p65 (Ser536) (Cell Signaling, 3033), rabbit anti–NF–κB p65 (Cell Signaling, 8242), and rabbit anti-actin (Cell Signaling, 4967) antibodies overnight at 4°C or for 2 h at room temperature (RT). The membranes were then washed with TBS containing 0.1% tween 20 (TBST) and incubated at RT for 1 h with the appropriate secondary antibodies conjugated to horseradish peroxidase (Jackson laboratories, 111-035-003 and 111-035-003). Enhanced chemiluminescent substrate (GenDEPOT, W3651-012) was used for visualization.

2.6. Confocal microscopy

To observe the subcellular localization of HMGB1, HEK293T, and HEK293-hTLR4A/MD2/CD14 cells were transfected with EGFP-tagged HMGB1 and $(HMGB1)_2$ for 36 h in LabTek II chambers (Nalgene, 154526 and 154534). Afterward, the cells were treated with 50 μM $CuCl_2$/50 μM H_2O_2 or 1 μg/mL LPS for 6 h, and washed with ice-cold PBS. The cells were fixed with 4% paraformaldehyde in PHEM buffer (60 mM PIPES, 5 mM HEPES, 10 mM EGTA, and 4 mM $MgSO_4$, pH 7.0) for 30 min at RT.

To investigate TLR4 oligomerization, RAW264.7 cells were incubated in LabTek II chambers with HMGB1 and $(HMGB1)_2$, which had been treated with 10 μM $CuCl_2$ and 50 μM H_2O_2 for 2 h, in the presence or absence of 5 mM DTT. The cells were then fixed in 4% paraformaldehyde, blocked with 1% BSA in PBS, and incubated with Alexa594-conjugated anti-mouse TLR4 antibody (R&D Systems, 1203B). After mounting with 4′,6′-diamidino-2-phenylindole (DAPI) (Vector Laboratories, H-1200-10), TLR4 oligomerization was visualized using confocal FV1000 microscopy (Olympus).

To determine which HMGB1 molecule could activate the cells, RAW264.7 cells were treated with 1 μg/mL of HMGB1 and $(HMGB1)_2$ in the presence or absence of DTT. The nuclear translocation of NF-κB p-p65 was then observed. The cells were fixed with 4% paraformaldehyde for 30 min, and permeabilized with 0.5% Triton X-100 for 20 min at RT. Following this, the cells were incubated with rabbit anti-p-p65 (Cell Signaling, 3033) at 4°C for 18 h, and then with Alexa594-conjugated goat anti-rabbit IgG antibody (Invitrogen, 111-585-144) as a secondary antibody.

2.7. Single-molecule pull-down assay

A single-molecular pull-down assay was conducted to confirm the orientation of HMGB1 when dimerized [13,48]. HEK293-hTLR4A/MD2/CD14 cells were transiently transfected with GFP^N-HMGB1 and either GFP^C-HMGB1 or HMGB1-GFP^C plasmids for 36 h and treated with 1 μg/mL LPS for 24 h. Cell culture supernatants were collected and concentrated using Amicon ultra centrifugal filters (Merck Millipore, UFC500396). These supernatants were then incubated with 50 μM H_2O_2 to induce HMGB1 dimerization. LabTek II chambers were coated with 0.01% poly-L-lysine (w/v) (Sigma Aldrich, P4707) in PBS at RT for 30 min, and after washing incubated with anti-GFP antibody (Abcam, ab5449) for 1 h. After blocking with 3% BSA-PBST, the supernatants were incubated at 4°C for 18 h. GFP fluorescence was observed under confocal FV1000 microscopy (Olympus).

2.8. Enzyme-linked immunosorbent assay

To compare the binding affinity of HMGB1 with TLR4/MD2 and TLR2 (Sino Biological, 10061-H08B), Di-HMGB1 was prepared. A 96-well PolySorp microtiter plate (Invitrogen™, 44-2404-21) was coated with 1 μg/mL of TLR proteins and blocked with 3% BSA-PBST. A two-fold dilution of HMGB1 starting from 10 μg/mL was added to the TLRs-coated plate and incubated at 4°C for 24 h. After washing with PBST, mouse anti-His antibody (Abcam, ab18184) was added with 1% BSA and incubated at 37°C for 1 h. After another round of washing, HRP-conjugated anti-mouse IgG (Jackson ImmunoResearch, 115-035-003) was incubated with 1% BSA at 37°C for 1 h. TMB solution was added after 5 washings, and the absorbance was measured at 450 nm.

2.9. Surface plasmon resonance analysis

To calculate the dissociation equilibrium constant (K_D) of HMGB1, $(HMGB1)_2$, and Di-HMGB1 with TLR4/MD2 and TLR2, we conducted an analysis using a Biacore™ T200 (GE Healthcare) instrument. For surface preparation, the recombinant hTLR4/MD2 complex and hTLR2 were immobilized on the CM5 sensor chip based on their molecular weights as the ligands. The CM5 sensor chip carries a matrix of carboxymethylated dextran covalently attached to a gold surface, in 10 mM sodium acetate buffer (pH 4.5). The surface of the CM5 sensor chip was activated with a mixture of 0.2 M 1-ethyl-3-(3-diethylaminopropyl)-carbodiimide and 0.05 M *N*-hydroxysuccinimide. HMGB1 and $(HMGB1)_2$ were serially diluted 2-fold from a 1.4 μM concentration and analyzed using HBS buffer (10 mM HEPES, 150 mM NaCl, 3.4 mM EDTA, and 0.005% Tween 20, pH 7.4). To evaluate binding, HMGB1 was passed over the sensor

chip. Real-time recording and analysis of sensorgrams were performed using the Biacore™ T200 system's control software. The data were then evaluated with the BIA evaluation Software (GE Healthcare).

2.10. HMGB1 secretion

To analyze the secreted HMGB1 in the culture supernatants, HEK293T and HEK293-hTLR4A/MD2/CD14 cell culture media were replaced with serum-free OPTI-MEM (Gibco™, 31985070) and transfected with Myc-tagged HMGB1, $(HMGB1)_2$, and $HMGB1^{C106A}$ plasmids for 36 h. HEK293T cells were treated with 50 μM $CuCl_2$ and 50 μM H_2O_2, whereas HEK293-hTLR4A/MD2/CD14 cells were treated with 1 μg/mL LPS for stimulation. After 18 h, each culture supernatant was incubated with 1 μg/mL LPS and 50 μM H_2O_2, respectively, and concentrated with a Centricon filter (Merck Millipore, UFC500396). Samples were subjected to SDS-PAGE in non-reducing conditions with or without 5 mM DTT.

2.11. Measurement of TNF-α

RAW264.7 and J774A.1 murine macrophage cells were cultured in 24-well plates at a density of 5×10^5 cells and 3×10^5 cells per well, respectively. Both cell types were treated with HMGB1, $(HMGB1)_2$, and $HMGB1^{C106A}$, which had been incubated with LPS and $CuCl_2/H_2O_2$ at 37°C for 2 h. To cleave the disulfide bond, 5 mM DTT was used, and to eliminate ROS, 50 μM NAC was employed. TNF-α concentration in the culture supernatants was determined using a sandwich enzyme-linked immunosorbent assay (ELISA) system (Invitrogen, 88-7324-88).

2.12. Mouse study

Animal studies were conducted using 7-8-week-old female C57BL/6 mice in accordance with procedures approved by the Institutional Animal Care and Use Committee of Yonsei Laboratory Animal Research Center (YLARC, 2018-0293). The mice were maintained under pathogen-free conditions with a 12:12 h light-dark cycle. To detect HMGB1 dimerization in the serum, the mice were intraperitoneally injected with 1 mg/kg LPS, and serum samples were collected 18 h after

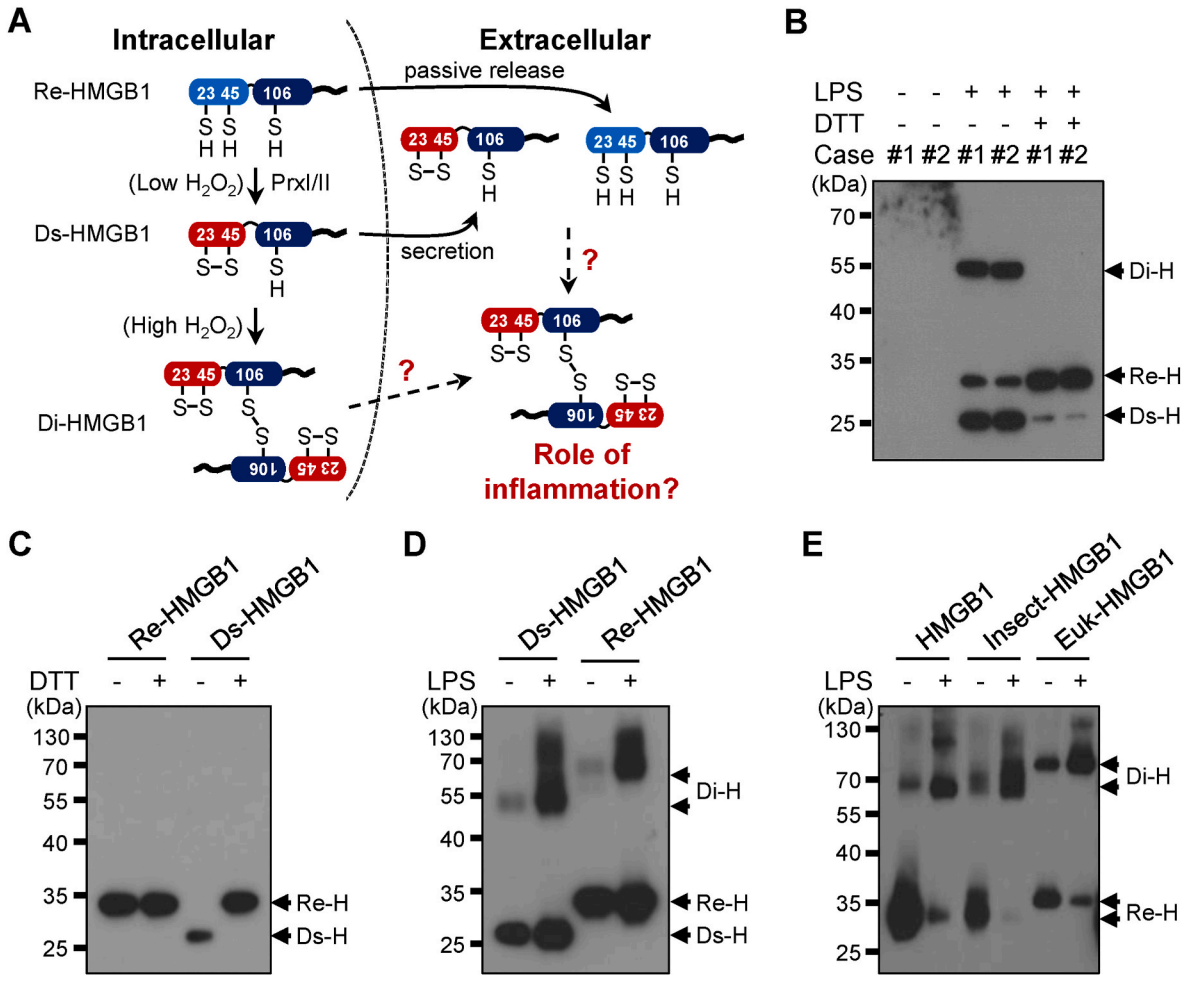

Fig. 1. Dimerization of HMGB1 *in vitro* and *in vivo*. (**A**) Study scheme: Different levels of ROS sequentially generated Ds-HMGB1 and Di-HMGB1 in the intracellular space. We investigated how Di-HMGB1 is formed in the extracellular space, whether Di-HMGB1 can be secreted, and what the pro-inflammatory function of Di-HMGB1 is in this study. (**B**) Two BALB/c mice were intraperitoneally injected with 1 mg/kg LPS. Blood samples were obtained after 24 h for non-reducing SDS-PAGE followed by immunoblotting with anti-HMGB1 antibody. Re-HMGB1 (Re–H), Ds-HMGB1 (Ds-H), and Di-HMGB1 (Di-H) were marked. (**C** and **D**) Re- and Ds-HMGB1 were purified and incubated with or without 5 mM DTT. Samples were separated using non-reducing SDS-PAGE for immunoblotting (**C**). Re- and Ds-HMGB1 (100 ng/μL) were incubated with 50 ng/mL LPS in normal mouse serum for 8 h at 37°C. Samples were diluted 20-fold and 100 ng of protein per well was separated using non-reducing SDS-PAGE (**D**). (**E**) Recombinant HMGB1 produced from *E. coli* (HMGB1), insect SF9 cells (Insect-HMGB1), and eukaryotic HEK293F cells (Euk-HMGB1) at 100 ng/μL were incubated with 50 ng/mL LPS in normal mouse serum for 8 h at 37°C. Samples were diluted and 100 ng of protein per well was separated using non-reducing SDS-PAGE for immunoblotting.

the LPS injection. HMGB1 dimerization was identified in 10-fold diluted serum using non-reducing SDS-PAGE.

2.13. Statistical analysis

Statistical analysis was performed using the Student's *t*-test in GraphPad Prism software version 5.0. All data represents the mean ± SEM of at least three individual measurements. The mean values are specified in the respective figure legends.

3. Results

3.1. Di-HMGB1 can be observed in extracellular space

PrxI and II induce the formation of a Cys^{23}-Cys^{45}-mediated intramolecular disulfide bond in HMGB1, known as Ds-HMGB1, under mild oxidative stress inside cells [23]. Excessive ROS in the nucleus can induce Cys^{106}-mediated intermolecular dimerization of HMGB1, referred to as Di-HMGB1, which helps protect against DNA damage (Fig. 1A) [13]. Through non-reducing SDS-PAGE analysis, both Ds-HMGB1 and Di-HMGB1 were detected in mouse serum samples that were obtained 24 h after intraperitoneal LPS injection, while no HMGB1 bands were detected in serum of LPS untreated mice (Fig. 1B). These results suggest that Di-HMGB1 can be formed from monomeric HMGB1

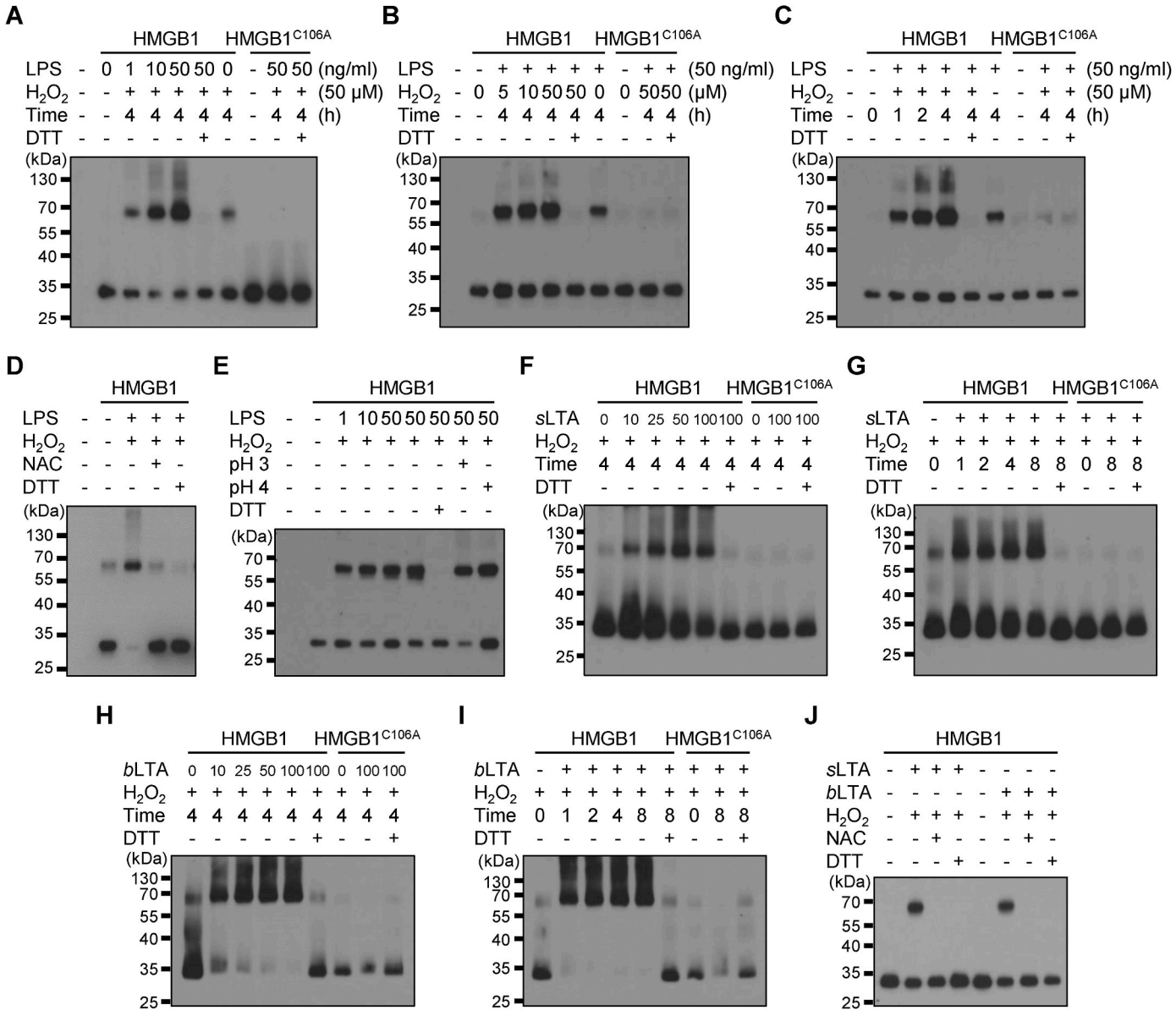

Fig. 2. Formation of Cys^{106}-mediated HMGB1 dimerization is facilitated by anchoring platforms in the presence of H_2O_2. (**A**–**C**) HMGB1 and $HMGB1^{C106A}$ at 100 ng/μL were incubated with various concentrations of LPS (**A**) and H_2O_2 (**B**), and various incubation times (**C**) in normal mouse serum at 37°C. (**D**) HMGB1 at 100 ng/μL was incubated with 20 ng/mL LPS and 50 μM H_2O_2 in normal mouse serum. 50 μM NAC or 5 mM DTT was used for 8 h at 37°C. (**E**) HMGB1 at 100 ng/μL was incubated with 50 μM H_2O_2 and different concentrations of LPS for 4 h at 37°C in normal mouse serum or citric buffered mouse serum at pH 3 and pH 4. (**F**–**I**) HMGB1 and $HMGB1^{C106A}$ at 100 ng/μL were incubated with various concentrations of *s*LTA and *b*LTA for 4 h at 37°C (**F**, **H**), or with various incubation time in the presence of 50 μM H_2O_2 (**G**, **I**). (**J**) HMGB1 at 100 ng/μL was incubated with 10 ng/mL *s*LTA or *b*LTA and 50 μM H_2O_2 in normal mouse serum. 50 μM NAC and 5 mM DTT were used to treat for 2 h at 37°C. Samples were diluted 20-fold and 100 ng of protein per well was separated using non-reducing SDS-PAGE for immunoblotting.

in the extracellular space. We further investigated the mechanism of Di-HMGB1 formation and its functional role.

For *in vitro* analysis of Di-HMGB1 formation, Re-HMGB1 and Ds-HMGB1 were produced in *E. coli* and purified, either in the presence or absence of DTT (Fig. 1C). Interestingly, Di-HMGB1 formation was observed when Re-HMGB1 and Ds-HMGB1 (100 ng/μL) were incubated with 50 ng/mL LPS in normal mouse serum (Fig. 1D). HMGB1 is known to bind well to LPS [25]. Di-HMGB1 formation was also observed with HMGB1 from various sources, including insect cells (Insect-HMGB1) and mammalian eukaryotic cells (Euk-HMGB1) when incubated with LPS in normal mouse serum (Fig. 1E). These results suggest that HMGB1 could be dimerized with the help of the binding platform of LPS in a cell-free environment.

3.2. Cys^{106}-mediated formation of Di-HMGB1

Di-HMGB1 was readily observed upon the addition of a binding ligand to HMGB1. We then investigated the mechanism underlying Di-HMGB1 formation. HMGB1 contains three cysteine residues (Cys^{23}, Cys^{45}, and Cys^{106}), with Cys^{23} and Cys^{45} involved in intramolecular disulfide bond formation [23,49]. To observe Di-HMGB1 formation in the extracellular space, HMGB1 and $HMGB1^{C106A}$ were incubated with LPS and H_2O_2 in normal mouse serum for 4 h at 37°C. Di-HMGB1 formation was observed in a dose-dependent manner with both LPS and H_2O_2 from HMGB1, but not from $HMGB1^{C106A}$, and increased with longer incubation times (Fig. 2A–C). NAC treatment reduced Di-HMGB1 formation (Fig. 2D). Low pH (pH 3 and pH 4), due to NAC's acidic carboxyl group with a pK_a of 3.14 [50], showed no effect on Di-HMGB1 formation (Fig. 2E).

In addition to LPS, the Gram-positive bacterial cell wall component LTA was used as an HMGB1 binding platform [30]. Di-HMGB1 was produced in a dose-dependent manner with both *s*LTA and *b*LTA in the presence of H_2O_2, whereas $HMGB1^{C106A}$ showed no formation (Fig. 2F–I). Additionally, NAC abolished HMGB1 dimerization (Fig. 2J). All these results indicate that HMGB1 could be dimerized via Cys^{106}-mediated interactions with pathogen-associated molecular pattern (PAMP) molecules such as LPS and LTA.

3.3. Dimerization of secreted HMGB1 in the opposite direction

Here, we investigated whether HMGB1 is secreted in a monomeric or dimeric form into the extracellular space. To do this, we used EGFP- or Myc-tagged HMGB1 and a $(HMGB1)_2$ plasmid for transfection (Fig. 3A) [13], where $(HMGB1)_2$ consists of two HMGB1 molecules linked by LK, mimicking Di-HMGB1. HEK293-hTLR4A/MD2/CD14 cells were overexpressed with Myc-tagged HMGB1 or $(HMGB1)_2$ for 24 h, followed by treatment with LPS for 18 h to collect the supernatant. This supernatant was then treated with 20 μM H_2O_2 for 4 h. Non-reducing immunoblotting revealed that monomeric HMGB1 was secreted and subsequently converted to Di-HMGB1 upon H_2O_2 treatment (Fig. 3B). When cells were overexpressed with $(HMGB1)_2$, neither secretion nor nucleocytoplasmic translocation of $(HMGB1)_2$ was observed, even after LPS treatment (Fig. 3B and C). Similarly, when HEK293T cells were subjected to oxidative stress (50 μM $CuCl_2$/50 μM H_2O_2) instead of LPS for 18 h, the results were consistent (Fig. 3D and E). The data suggest that HMGB1 is secreted as a monomer and dimerized into Di-HMGB1 under LPS or oxidative treatment in the supernatants.

Next, we performed a single-molecule pull-down assay to verify the binding orientation of two HMGB1 molecules in Di-HMGB1. Bimolecular fluorescence complementation (BiFC) constructs, consisting of GFP^N-HMGB1 and either GFP^C-HMGB1 or HMGB1-GFP^C, were co-transfected into HEK293-hTLR4A/MD2/CD14 cells. The cells were then exposed to LPS to induce HMGB1 secretion. The culture supernatants from cells overexpressing GFP^N-HMGB1 and HMGB1-GFP^C showed a GFP signal, which was intensified with 50 μM H_2O_2 (Fig. 3F and G). These results indicate that two HMGB1 proteins form a dimer in an antiparallel orientation in the extracellular space under oxidative conditions.

3.4. Di-HMGB1 binds to TLR4/MD2 and TLR2 stronger than HMGB1

Extracellular HMGB1 binds to TLR4 and mediates NF-κB signaling [51]. The Cys^{106} residue of HMGB1 is a critical residue for HMGB1-TLR4 binding [43]. Co-treatment with HMGB1 and PAMPs, such as LPS, LTA, and CpG complex, synergistically induces cytokine production compared to treatment with either HMGB1 or PAMPs alone [25,30,52]. To investigate the effect of Di-HMGB1 on NF-κB signaling, we first measured the binding affinity of Di-HMGB1 to TLR4. Di-HMGB1 and oligomeric HMGB1 were produced by incubating HMGB1 with 10 μM $CuCl_2$ and 50 μM H_2O_2 for 18 h [13], resulting in approximately 64.7% of Di-HMGB1 and oligomeric HMGB1 as determined by the ImageJ program (Fig. 4A). Microtiter plates were coated with the TLR4/MD2 complex, and equal amounts of HMGB1 and Di-HMGB1 were added to the wells. Both HMGB1 and Di-HMGB1 exhibited dose-dependent binding to the TLR4/MD2 complex, with Di-HMGB1 showing stronger binding than that of HMGB1. However, mutant $HMGB1^{C106A}$, which is known to not bind to TLR4/MD2, displayed no binding to the TLR4/MD2 complex (Fig. 4B).

Immunoprecipitation studies demonstrated that Di-HMGB1 bound to TLR4/MD2 complexes more effectively than HMGB1 at the same concentration, whereas $HMGB1^{C106A}$ showed no binding (Fig. 4C). Next, recombinant 6xhis-tagged $(HMGB1)_2$ was produced and purified to further confirm the effect of Di-HMGB1 (Fig. 4D). HMGB1, $(HMGB1)_2$, and Di-HMGB1 were then applied to a CM5 dextran sensor chip immobilized with TLR4/MD2. The sensograms demonstrated that HMGB1, $(HMGB1)_2$, and Di-HMGB1 bound to TLR4/MD2 in a dose-dependent manner, with K_D values of 2.986×10^{-7} M, 2.100×10^{-7} M, and 8.600×10^{-8} M, respectively (Fig. 4E–G). $HMGB1^{C106A}$ did not bind to TLR4/MD2, consistent with a previous report [43] (Suppl. Fig. 1). Additionally, $CuCl_2/H_2O_2$-treated $(HMGB1)_2$ showed stronger TLR4 oligomerization compared to $CuCl_2/H_2O_2$-treated HMGB1 at the same concentration in RAW264.7 cells, as observed by confocal microscopy (Fig. 4H). When examining the binding of HMGB1, $(HMGB1)_2$, and Di-HMGB1 to TLR2, $(HMGB1)_2$ and Di-HMGB1 exhibited stronger binding to TLR2 than monomeric HMGB1 in both ELISA and SPR assay (Fig. 4I–L). The K_D values for HMGB1, $(HMGB1)_2$, and Di-HMGB1 and binding to TLR2 were 4.956×10^{-7} M, 1.772×10^{-7} M, and 1.523×10^{-8} M, respectively. Collectively, these findings indicate that dimeric HMGB1 binds more strongly to TLR4 and TLR2 receptors than monomeric form. HMGB1 could bind LPS and deliver it into the cytosol for the activation of caspase 11 via RAGE [53]. We observed the effect of Di-HMGB1 binding to RAGE. The binding of Di-HMGB1 to RAGE and its oligomerization were enhanced compared to monomeric HMGB1 (Suppl. Fig. 2).

3.5. Di-HMGB1 induces strong NF-κB signaling

To compare the effects of HMGB1 and Di-HMGB1 on pro-inflammatory signaling, we observed the levels of phosphorylated-p65 (p-p65) in RAW264.7 cells after treatment with both forms of HMGB1. Both $CuCl_2/H_2O_2$-treated HMGB1 and $(HMGB1)_2$ significantly induced higher p-p65 levels compared to non-treated controls (Fig. 5A–C). Treatment with the antioxidant NAC and the reducing agent DTT reduced the p-p65 induction by $CuCl_2/H_2O_2$-treated HMGB1 and $(HMGB1)_2$ to baseline levels (Fig. 5A and B). Additionally, $CuCl_2/H_2O_2$-treated $(HMGB1)_2$, which forms a Cys^{106}-Cys^{106} bond, exhibited a stronger p-p65 induction than that of monomeric HMGB1 (Fig. 5C). When RAW264.7 cells were co-treated with LPS and either HMGB1 or $(HMGB1)_2$ in the presence or absence of H_2O_2, the levels of p-p65 were significantly increased in the presence of H_2O_2 (Fig. 5D and E). HMGB1 enhances pro-inflammatory cytokine production by facilitating the transfer of LPS to CD14 [25]. Confocal microscopy showed that the

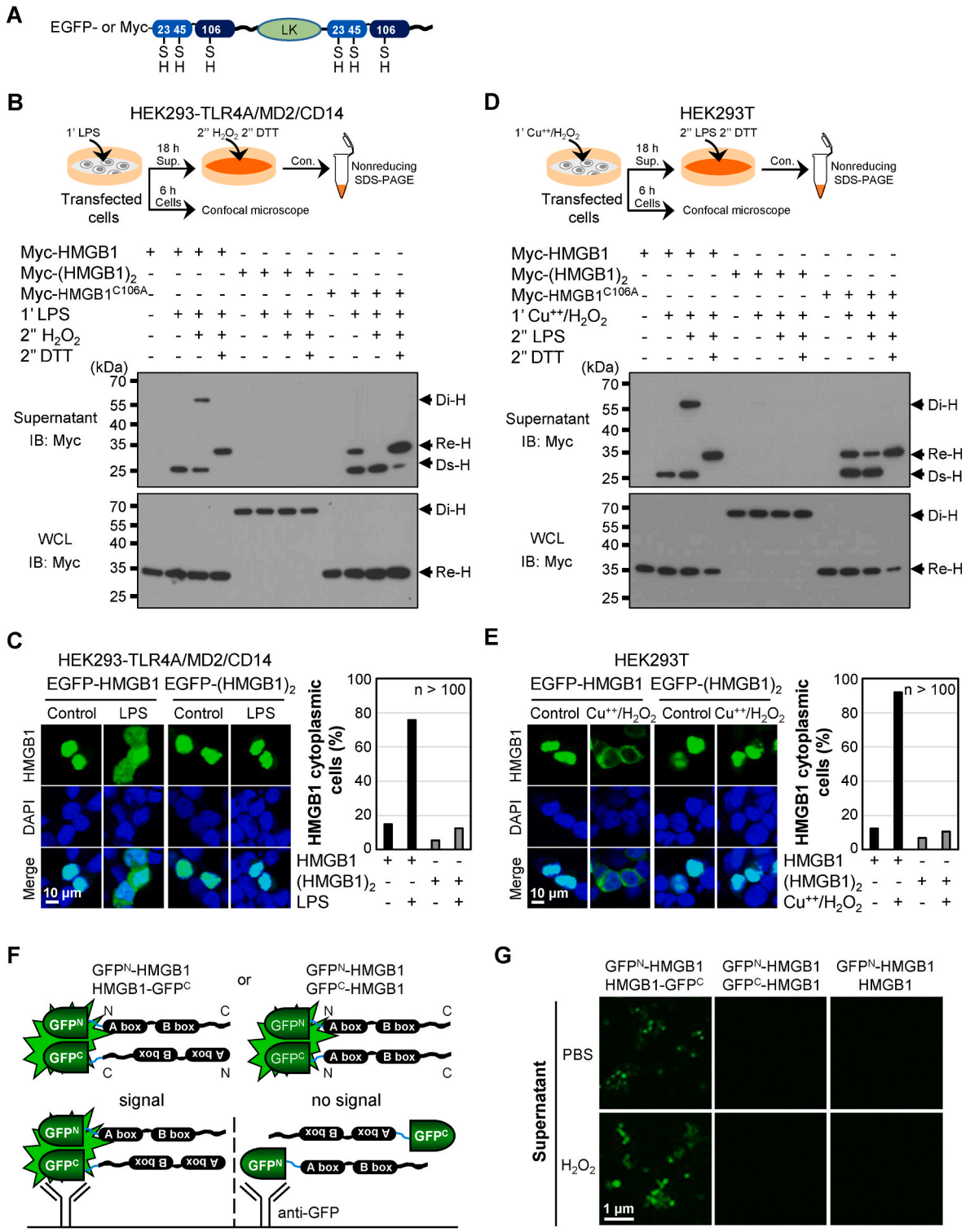

Fig. 3. HMGB1 secretion and its dimerization in the extracellular space. (**A**) Cartoon depicting $(HMGB1)_2$ construct. (**B**) HEK293-hTLR4A/MD2/CD14 cells were transfected with Myc-tagged HMGB1, $(HMGB1)_2$, and $HMGB1^{C106A}$ plasmids for 24 h. The cells were stimulated with 1 μg/mL LPS for 18 h. The supernatants were harvested and treated with 50 μM $CuCl_2$/50 μM H_2O_2 for 4 h, followed by non-reducing SDS-PAGE and immunoblotting. Sup., supernatant; Con., concentration; WCLs, Whole cell lysates. (**C**) HEK293-hTLR4A/MD2/CD14 cells were transfected with each plasmid for 24 h and treated with LPS for 6 h for confocal microscopy. (**D**) HEK293T cells were transfected with each plasmid for 24 h and stimulated 50 μM $CuCl_2$/50 μM H_2O_2 for 18 h. The supernatants were treated with LPS and DTT for 4 h followed by non-reducing SDS-PAGE and immunoblotting. (**E**) HEK293T cells were transfected with each plasmid for 24 h and then stimulated with 50 μM $CuCl_2$/50 μM H_2O_2 for 6 h. EGFP fluorescence was observed by confocal microscopy. The percentage of cytoplasmic EGFP-HMGB1 was determined by counting over 100 cells (**C** and **E**). (**F** and **G**) Single-molecule pull-down assay using bimolecular fluorescence complementation (BiFC) signal (**F**). HEK293-TLR4A/MD2/CD14 cells were co-overexpressed with both GFP^N-HMGB1 and HMGB1-GFP^C or GFP^C-HMGB1 plasmids for 24 h and treated with 1 μg/mL LPS for 18 h. The culture supernatants were harvested and incubated on LabTek II chambers coated with anti-GPF antibody in the presence or absence of 50 μM H_2O_2. H_2O_2 was added to the supernatants for HMGB1 dimerization. BiFC signal of GFP was observed under confocal microscopy. Co-transfection of both GFP^N-HMGB1 and HMGB1 plasmids was used as a negative control (**G**).

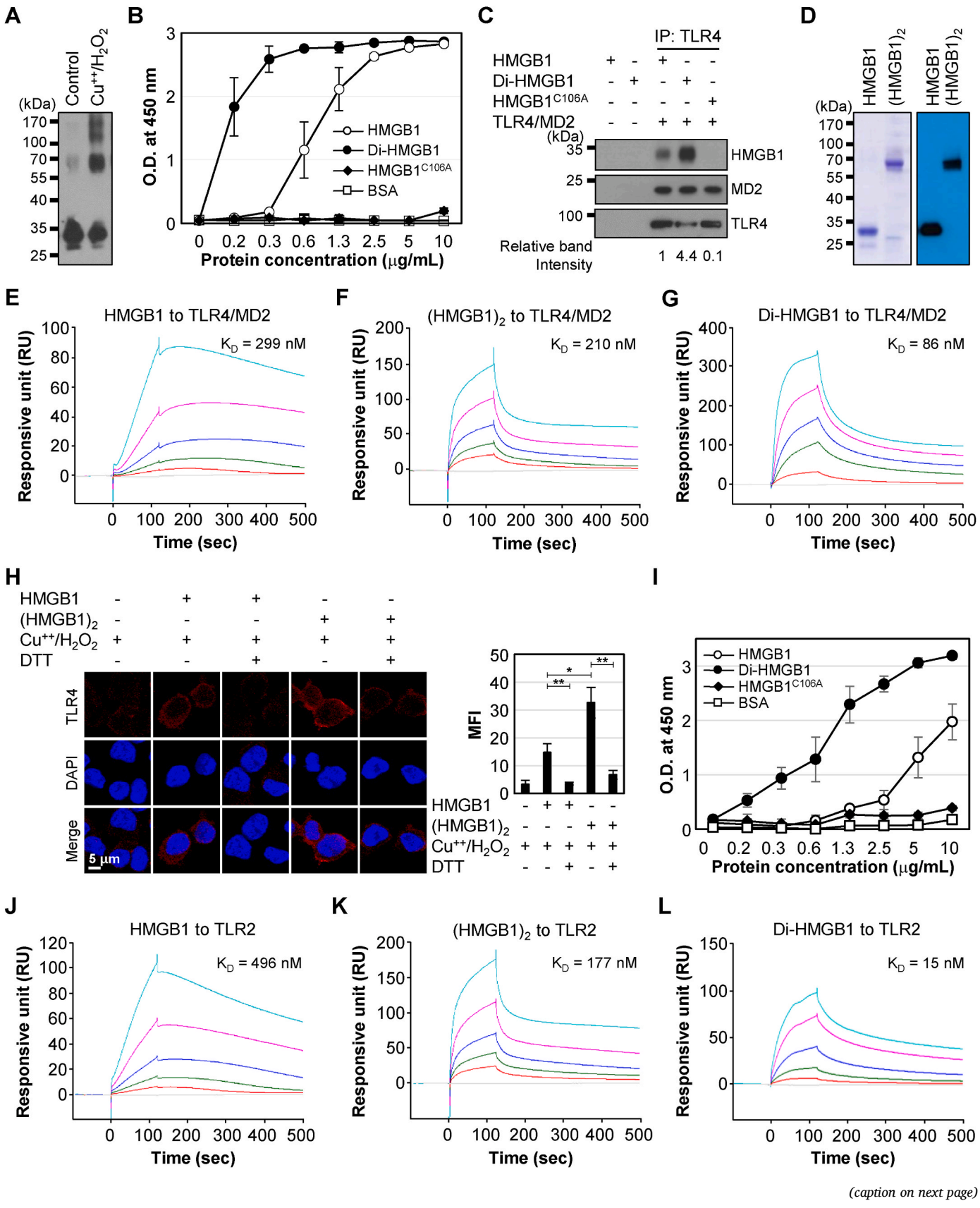

(caption on next page)

Fig. 4. Di-HMGB1 binding to TLR4/MD2 and TLR2. (**A**) Di-HMGB1 was produced by incubating HMGB1 with 10 μM $CuCl_2$ and 50 μM H_2O_2 for 18 h at 37°C. (**B**) The TLR4/MD2 complex (1 μg/mL) was coated on a polystyrene microplate for 18 h at 4°C. HMGB1, Di-HMGB1, and $HMGB1^{C106A}$ proteins were then serially diluted and used for ELISA. BSA was used as a control protein. N = 3. (**C**) The TLR4/MD2 complex (400 ng/mL) was incubated with various HMGB1 proteins (each 100 ng/mL) for 2 h at 37°C. The mixture was then immunoprecipitated with an anti-TLR4 antibody for immunoblotting using anti-HMGB1, anti-MD2, and anti-TLR4 antibodies. The relative band intensities of HMGB1/MD2 were calculated using ImageJ software (NIH). (**D**) His_6-tagged HMGB1 and $(HMGB1)_2$ proteins were produced in *E. coli*. The proteins were observed at the expected size by Coomassie blue staining (left) and Western blotting (right) after SDS-PAGE. (**E**–**G**) SPR analysis was conducted to study HMGB1 binding to TLR4/MD2. HMGB1 (**E**), $(HMGB1)_2$ (**F**) and Di-HMGB1 (**G**) were serially diluted starting from 1.4 μM and flowed over TLR4/MD2-immobilized CM5 dextran sensor chip. (**H**) Confocal analysis showing TLR4 oligomerization in RAW264.7 cells. The cells were treated with HMGB1 and $(HMGB1)_2$, which had been incubated with 10 μM $CuCl_2$ and 50 μM H_2O_2 for 2 h, in the presence or absence of 5 mM DTT. TLR4 was stained with Alexa594-conjugated anti-mouse TLR4 antibody. The fluorescence intensity was calculated using ImageJ software, and the mean fluorescence intensity (MFI) was presented as mean ± SEM (N = 3). *p < 0.01, **p < 0.001, *t*-test. (**I**) TLR2 (1 μg/mL) was coated on a polystyrene microplate for 18 h at 4°C. Serially diluted HMGB1, Di-HMGB1, and $HMGB1^{C106A}$ mutant proteins were added and binding was evaluated by ELISA, with BSA as a control protein. N = 3. (**J**–**L**) SPR analysis of HMGB1 binding to TLR2. HMGB1 (**J**), $(HMGB1)_2$ (**K**), and Di-HMGB1 (**L**) were flowed over TLR2-immobilized CM5 dextran sensor chip. HMGB1 and $(HMGB1)_2$ were serially diluted starting from 1.4 μM and flowed over TLR4/MD2-immobilized CM5 dextran sensor chip.

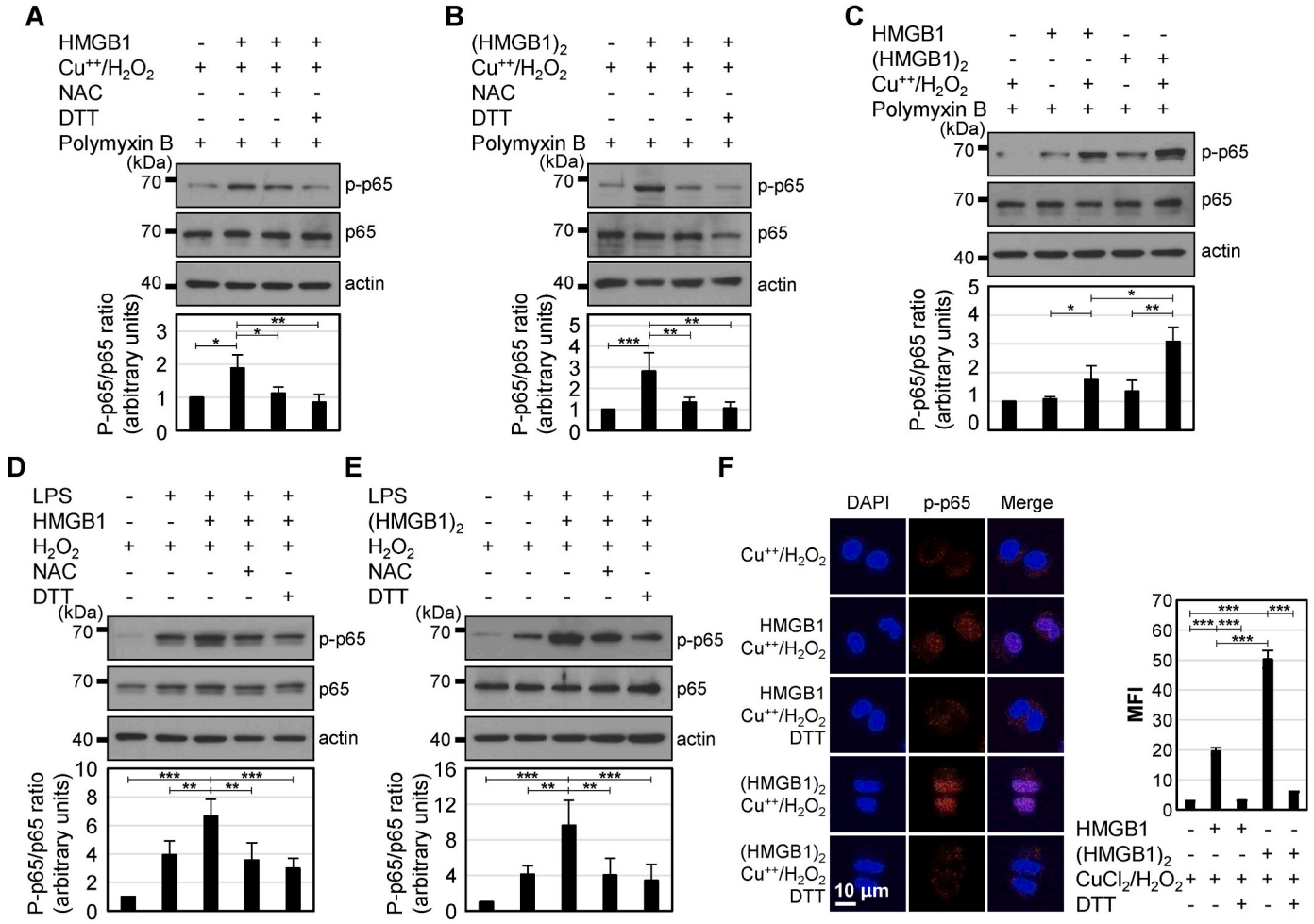

Fig. 5. Di-HMGB1 induces strong NF-κB signaling. (**A** and **B**) HMGB1 (**A**) and $(HMGB1)_2$ (**B**) were incubated with 10 μM $CuCl_2$ and 50 μM H_2O_2 in the presence or absence of 50 μM NAC or 5 mM DTT for 2 h and then treated on RAW264.7 cells for 30 min. Whole-cell lysates (WCLs) were immunoblotted with anti-p-p65, anti-p65, and anti-β-actin antibodies after SDS-PAGE analysis. The p-p65/p65 ratio was compared. Polymyxin B was used to neutralize endotoxin. (**C**) RAW264.7 cells were treated with HMGB1 and $(HMGB1)_2$ for 30 min, which were prepared as like (**A**) and (**B**) in the presence or absence of 10 μM $CuCl_2$ and 50 μM H_2O_2 for 2 h. (**D** and **E**) HMGB1 (**D**) and $(HMGB1)_2$ (**E**) were incubated with 10 ng/mL LPS and 50 μM H_2O_2 in the presence or absence of 50 μM NAC or 5 mM DTT for 2 h and then treated on RAW264.7 cells for 30 min. All band intensities were calculated using ImageJ software and presented as the mean ± SEM (N = 3). *p < 0.05, **p < 0.01, ***p < 0.001. (**F**) HMGB1 and $(HMGB1)_2$ were incubated with 10 μM $CuCl_2$ and 50 μM H_2O_2 in the presence or absence of 5 mM DTT for 2 h and then treated on RAW264.7 cells for 30 min. Cells were permeabilized and incubated with an anti-p-p65 antibody for confocal microscopy. Mean fluorescence intensity (MFI) was presented as mean ± SEM (N = 3). ***p < 0.001, *t*-test. Nuclei were stained with DAPI.

nuclear translocation of p-p65 was more pronounced following treatment with $(HMGB1)_2$ compared to HMGB1 at the same concentration (Fig. 5F). These results suggest that the formation of Di-HMGB1 under high oxidative stress induces stronger TLR4/MD2-mediated signaling compared to monomeric HMGB1.

3.6. Di-HMGB1 enhances TNF-α production

Next, we assessed the effect of $CuCl_2/H_2O_2$-treated HMGB1 and $(HMGB1)_2$ on TNF-α production in RAW264.7 cells. Both $CuCl_2/H_2O_2$-treated HMGB1 and $(HMGB1)_2$ induced TNF-α production in a dose-

dependent manner compared to untreated controls (Fig. 6A). $CuCl_2$/H_2O_2-treated $(HMGB1)_2$ significantly increased TNF-α production compared to monomeric HMGB1, and this effect was abolished by DTT and NAC (Fig. 6A and B). These data suggest that the presence of Di-HMGB1 is crucial in the pro-inflammatory response. Co-treatment of either H_2O_2-treated HMGB1 or $(HMGB1)_2$ with LPS led to higher TNF-α production than LPS alone, and these pro-inflammatory effects were reduced by DTT and NAC (Fig. 6C and D). The $HMGB1^{C106A}$ mutant failed to induce TNF-α production (Fig. 6A–D).

Finally, we produced Di-HMGB1 by incubating HMGB1 with 50 μM H_2O_2 and 10 ng/mL LPS, *s*LTA and *b*LTA for 1 h and 17 h, referred to as HMGB1/H_2O_2/LPS-1 or -17 and HMGB1/H_2O_2/LTA-1 or -17. After 17 h of incubation, HMGB1 molecules were dimerized or oligomerized by approximately 70–90% (Fig. 7A–C). When RAW264.7 and J774A.1 cells were treated with HMGB1/H_2O_2/LPS-17 for 2 h, TNF-α levels in the culture supernatant increased dose-dependently, significantly more than those treated with LPS or LTA alone. Additionally, TNF-α levels in the culture supernatant with HMGB1/H_2O_2/LPS-17 were significantly increased compared to HMGB1/H_2O_2/LPS-1 treatment (Fig. 7D and E). Similarly, HMGB1/H_2O_2/*s*LTA and HMGB1/H_2O_2/*b*LTA stimulations produced similar results (Fig. 7F–I). All these results indicate that the amount of Di-HMGB1 stimulation produces a strong pro-inflammatory response.

In summary, extracellular HMGB1 is secreted in monomer form by pro-inflammatory stimuli and efficiently forms a dimeric structure in an anti-parallel orientation mediated by Cys^{106}-Cys^{106} under oxidative conditions. This dimerization is facilitated by anchoring platforms such as LPS and LTA. These Di-HMGB1 molecules bind more effectively to TLR4/MD2 and TLR2, delivering NF-κB signaling for TNF-α production more robustly than monomeric HMGB1 (Fig. 8). These results elucidate a new paradigm in the pathogenesis of HMGB1-mediated inflammation in both sterile and septic conditions.

4. Discussion

HMGB1 is a redox-sensitive protein containing three cysteine residues Cys^{23}, Cys^{45}, and Cys^{106}. PrxI/II can induce the formation of an intramolecular disulfide bond between Cys^{23} and Cys^{45} residues of HMGB1 in the nucleus under mild oxidative stress. This Ds-HMGB1 is then translocated into the cytoplasm for secretion [23]. It is known that the Cys^{23}-Cys^{45} intramolecular disulfide bond and the Cys^{106} thiol form are required for HMGB1 to induce pro-inflammatory cytokines [21,43]. Our recent study recently showed that HMGB1 dimerization via the Cys^{106}-Cys^{106} intermolecular disulfide bond prevents DNA damage from oxidative stress in the nucleus [13]. This demonstrates the formation of Di-HMGB1 and its physiological role in cellular stress.

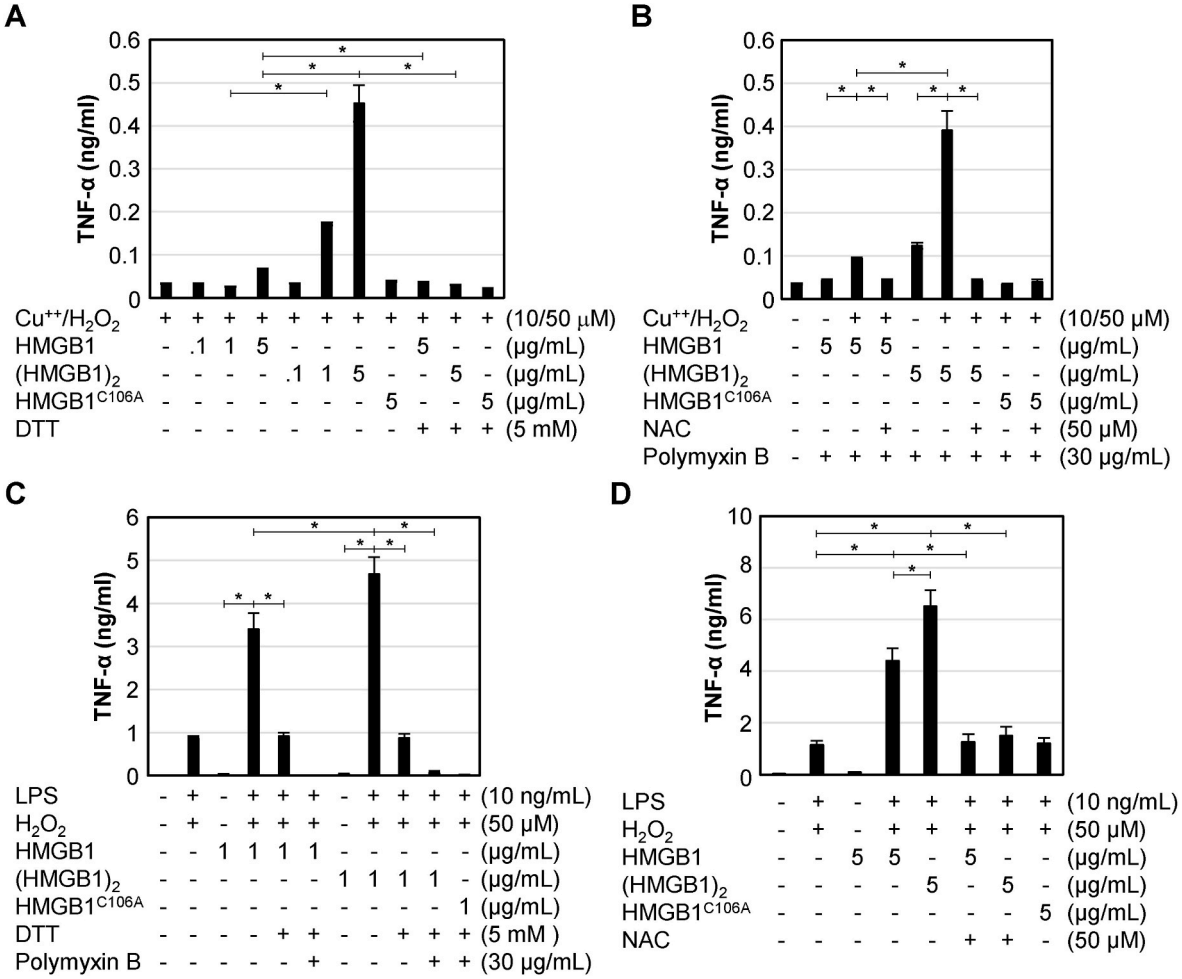

Fig. 6. Di-HMGB1 enhances TNF-α production. (A and **B**) HMGB1, $(HMGB1)_2$, and $HMGB1^{C106A}$ were incubated with 10 μM $CuCl_2$ and 50 μM H_2O_2 in the presence or absence of 5 mM DTT (**A**) or 50 μM NAC (**B**). RAW264.7 cells were stimulated with the indicated amount of HMGB1, $(HMGB1)_2$, and $HMGB1^{C106A}$ mixture for 2 h. Polymyxin B was used for endotoxin removal. (**C** and **D**) HMGB1, $(HMGB1)_2$, and $HMGB1^{C106A}$ were incubated with or without 10 ng/mL LPS and 50 μM H_2O_2 in the presence or absence of 5 mM DTT (**C**) or 50 μM NAC (**D**). RAW264.7 cells were stimulated with the indicated amount of HMGB1, $(HMGB1)_2$, and $HMGB1^{C106A}$ mixture. Supernatants were collected after 2 h of treatment and TNF-α levels were quantified using a commercial ELISA kit. *$p < 0.001$ vs $(HMGB1)_2$ by two-way ANOVA followed by Tukey's test.

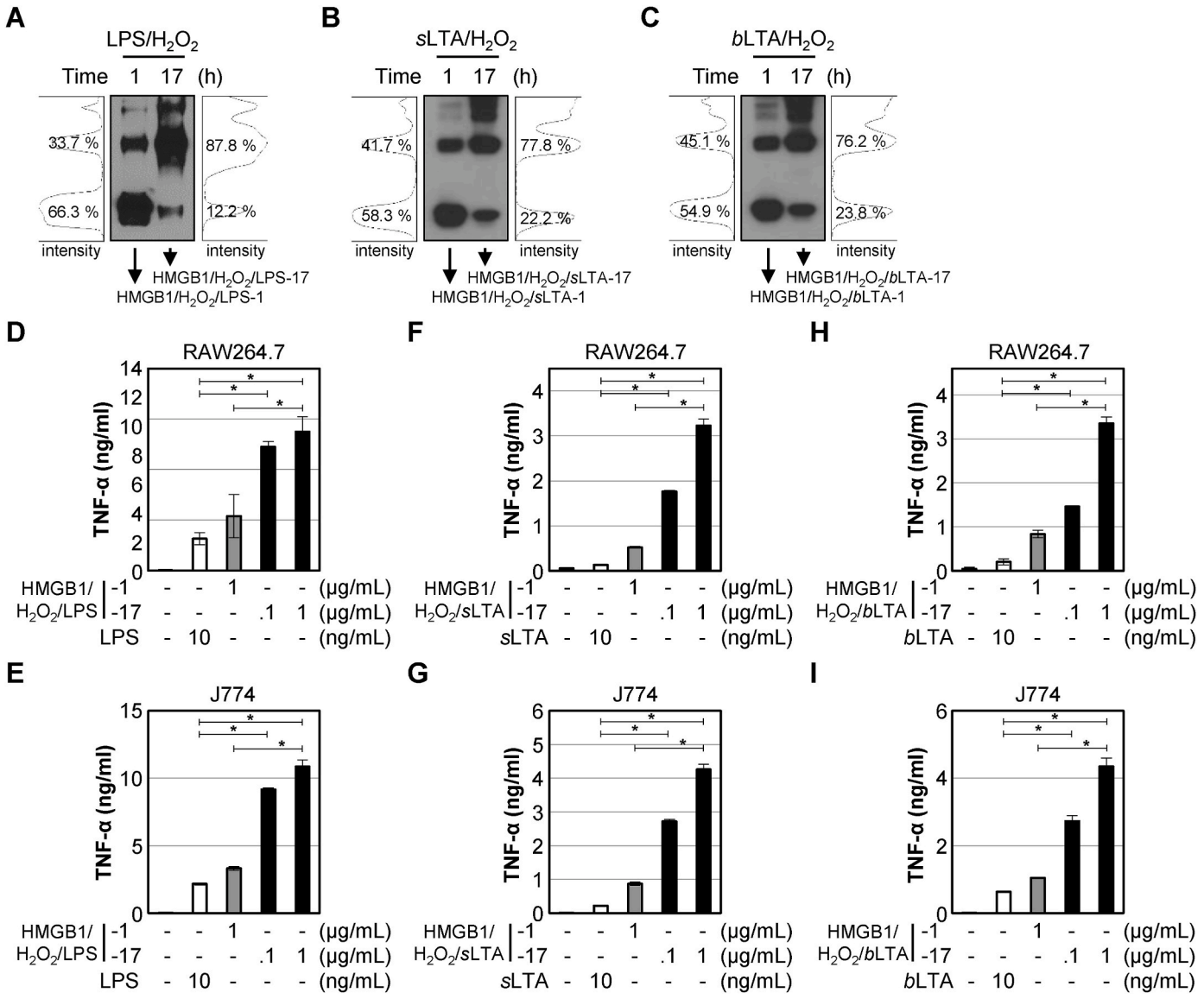

Fig. 7. Di-HMGB1 formed from monomeric HMGB1 enhances TNF-α production. (A–**C**) Various concentrations of HMGB1 dimeric forms were produced by incubation with 50 μM H_2O_2 and 10 ng/mL LPS from *Escherichia coli* 0111:B4 (**A**) or LTA from *Staphylococcus aureus* (**B**, *s*LTA) or *Bacillus subtilis* (**C**, *b*LTA) for 1 or 17 h at 37°C. Percentages of band intensities were calculated using ImageJ software (NIH). (**D**–**I**) RAW264.7 (**D**, **F**, **H**) and J774A.1 (**E**, **G**, **I**) cells were stimulated with 0.1 or 1 μg/mL of HMGB1 mixture incubated with LPS (**D**, **E**) or *s*LTA (**F**, **G**), or *b*LTA (**H**, **I**) for 2 h. Supernatants were collected and TNF-α levels were quantified using a commercial ELISA kit. Stimulation with 10 ng/mL of LPS (**D**, **E**) or *s*LTA (**F**, **G**) or *b*LTA (**H**, **I**) was used as a positive control. *$p < 0.001$ vs PAMPs incubated-Di-HMGB1 by two-way ANOVA followed by Tukey's test.

In this study, we found that HMGB1 is secreted extracellularly in the monomeric form and can be dimerized into Di-HMGB1 under oxidative conditions with the aid of binding platforms such as LPS and LTA. HMGB1 proteins in Di-HMGB1 are dimerized in an anti-parallel direction. Di-HMGB1 exhibited a higher binding affinity to TLR4, TLR2, and RAGE than to monomeric HMGB1. Treatment with $(HMGB1)_2$, the mimic form of Di-HMGB1, resulted in strong TLR4 oligomerization, increased nuclear p-p65, activation of NF-κB signaling, and elevated TNF-α production. TLR2, TLR4, and RAGE are known to be oligomerized by their respective ligands to activate signaling, leading to the recruitment of downstream signaling molecules [33,35,54,55]. Therefore, extracellular HMGB1 dimerization or oligomerization under oxidative stress is crucial for the inflammatory reaction. Ligand oligomerization enhances the corresponding receptor oligomerization for improved signaling pathways. For example, S100B, a RAGE receptor ligand, forms a tetramer with a greater binding affinity for RAGE than its monomeric form. Additionally, the RagA pneumococcal pilus type 1 protein can oligomerize to effectively bind to TLR2 [36,38,39]. This is why treatment with fresh recombinant monomeric HMGB1 showed low pro-inflammatory cytokine production both *in vitro* and *in vivo*. This study represents the first report on the extracellular dimerization of HMGB1, which triggers strong pro-inflammatory signaling through receptor oligomerization. We are currently investigating the role of Di-HMGB1 in intracellular signaling after RAGE-dependent endocytosis, which has important implications for caspase-11-dependent lethality in sepsis [53].

A previous report demonstrated that Ds-HMGB1, which contains the free thiol group of Cys^{106}, induces TLR4-mediated pro-inflammatory signaling through Cys^{106}-mediated binding to TLR4 [43]. The absence of the Cys^{106} thiol in HMGB1 abolishes these pro-inflammatory effects. Although the specific mechanism by which the Cys^{106} thiol of HMGB1 is required to induce pro-inflammatory signals via TLR4 has not been identified, our study shows that Di-HMGB1, which contains a Cys^{106}-mediated disulfide bond and lacks a free thiol, still exhibits

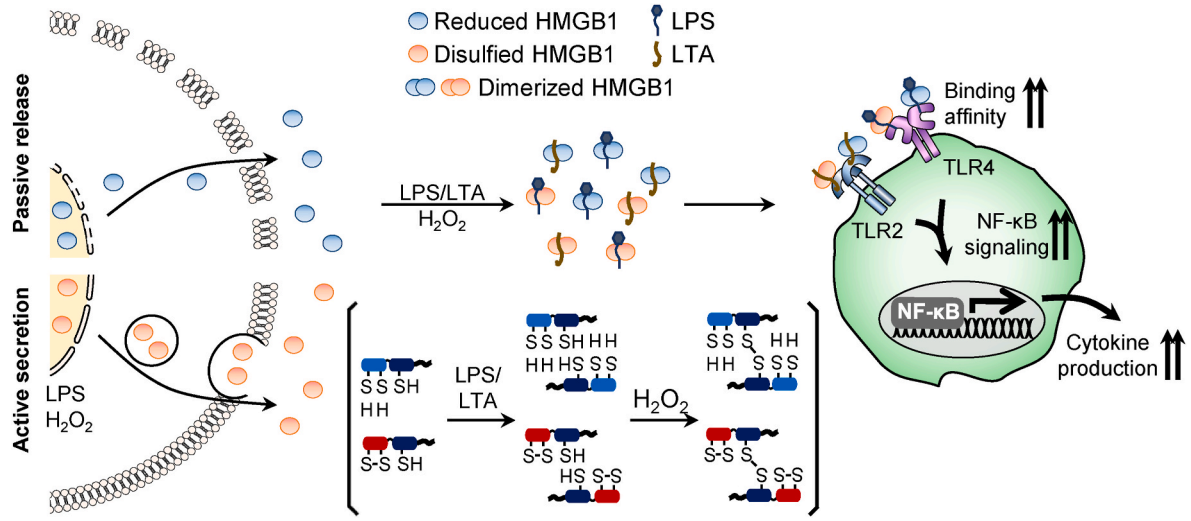

Fig. 8. A model for PAMPs/H_2O_2-mediated HMGB1 homo-dimerization and its pro-inflammatory effects. Passively released extracellular HMGB1, mostly in reduced form, and actively secreted extracellular HMGB1, predominantly in a disulfide form, are initially secreted as monomers. These monomeric forms of HMGB1 can undergo self-association on platforms such as LPS and LTA. The presence of ROS facilitates this process through Cys^{106}-Cys^{106}-mediated anti-parallel inter-molecular dimerization. The resulting Di-HMGB1 exhibits increased binding affinity for TLR4 and TLR2, enhances NF-κB signaling, and elevates TNF-α production compared to monomeric HMGB1.

binding affinity for TLR4 and TLR2, contributing to pro-inflammatory signaling. Furthermore, the reduction of Di-HMGB1 via DTT treatment decreases its binding affinity to the TLR4 receptor, p-p65 formation, and TNF-α production. Additionally, the degree of HMGB1 dimerization correlates with ROS levels [13], and the levels of ROS generation and HMGB1 oxidation correspond to the severity of sepsis [56].

We do not yet have a definitive explanation for why HMGB1, lacking a free thiol group at Cys^{106}, such as in Di-HMGB1, can bind to TLR4/MD2. TLR4 primarily utilizes hydrophobic or ionic interactions when binding to its partners such as MD2, CD14, and LPS, but does not bind its ligand via intermolecular disulfide bond formation to the best of our knowledge [57,58]. Considering that sulfonylated HMGB1, which has the $–SO_3$ group at Cys23, 45, and 106, was bound to MD2 with K_D of 25 μM [59], Di-HMGB1 containing Cys-Cys bond did not significantly affect the interaction with TLR4/MD2. Further in-depth investigation is required to explore this phenomenon in detail.

Overall, these results suggest that Di-HMGB1 may form in extracellular spaces under oxidative conditions and play an important pro-inflammatory role as a DAMP. Further analysis is required to detect Di-HMGB1 in human septic patients and evaluate the disease severity. The development of an assay to detect Di-HMGB1 in samples is crucial for clinical diagnosis and treatment.

CRediT authorship contribution statement

Man Sup Kwak: Writing – review & editing, Writing – original draft, Supervision, Funding acquisition, Formal analysis, Data curation, Conceptualization. **Myeonggil Han:** Writing – original draft, Formal analysis, Data curation. **Yong Joon Lee:** Methodology, Data curation. **Seoyeon Choi:** Writing – review & editing, Data curation. **Jeonghwa Kim:** Investigation, Formal analysis. **In Ho Park:** Methodology, Investigation, Formal analysis. **Jeon-Soo Shin:** Writing – review & editing, Writing – original draft, Validation, Supervision, Project administration, Funding acquisition, Data curation, Conceptualization.

Funding

This study was supported by grants from the National Research Foundation of Korea (NRF), funded by the Korean government [RS-2019-NR040072 and RS-2022-NR068972 to JSS, and 2021R1I1A1A01044809 to MSK], and Research Center Program of the Institute for Basic Science (IBS) in Korea [IBS-R026-D1] to JSS.

Declaration of competing interest

The authors declare that they have no known competing financial interests or personal relationships that could have appeared to influence the work reported in this paper.

Acknowledgments

None.

Appendix A. Supplementary data

Supplementary data to this article can be found online at https://doi.org/10.1016/j.redox.2025.103521.

Data availability

Data will be made available on request.

References

[1] X. Lin, J. Liu, F. Maley, E. Chu, Role of cysteine amino acid residues on the RNA binding activity of human thymidylate synthase, Nucleic Acids Res. 31 (16) (2003) 4882–4887, https://doi.org/10.1093/nar/gkg678.
[2] S.F. Arnold, D.P. Vorojeikina, A.C. Notides, Phosphorylation of tyrosine 537 on the human estrogen receptor is required for binding to an estrogen response element, J. Biol. Chem. 270 (50) (1995) 30205–30212, https://doi.org/10.1074/jbc.270.50.30205.
[3] J.P. Changeux, S.J. Edelstein, Allosteric mechanisms of signal transduction, Science (New York, N.Y.) 308 (5727) (2005) 1424–1428, https://doi.org/10.1126/science.1108595.
[4] I.M. Nooren, J.M. Thornton, Structural characterisation and functional significance of transient protein-protein interactions, J. Mol. Biol. 325 (5) (2003) 991–1018, https://doi.org/10.1016/s0022-2836(02)01281-0.
[5] S.R. Devenish, J.A. Gerrard, The role of quaternary structure in (beta/alpha)(8)-barrel proteins: evolutionary happenstance or a higher level of structure-function relationships? Org. Biomol. Chem. 7 (5) (2009) 833–839, https://doi.org/10.1039/b818251p.
[6] S.M. Simon, F.J. Sousa, R. Mohana-Borges, G.C. Walker, Regulation of Escherichia coli SOS mutagenesis by dimeric intrinsically disordered umuD gene products, Proc. Natl. Acad. Sci. U. S. A. 105 (4) (2008) 1152–1157, https://doi.org/10.1073/pnas.0706067105.

[7] J.H. Fong, B.A. Shoemaker, S.O. Garbuzynskiy, M.Y. Lobanov, O.V. Galzitskaya, A. R. Panchenko, Intrinsic disorder in protein interactions: insights from a comprehensive structural analysis, PLoS Comput. Biol. 5 (3) (2009) e1000316, https://doi.org/10.1371/journal.pcbi.1000316.

[8] M. Bustin, R. Reeves, High-mobility-group chromosomal proteins: architectural components that facilitate chromatin function, Prog. Nucleic Acid Res. Mol. Biol. 54 (1996) 35–100, https://doi.org/10.1016/s0079-6603(08)60360-8.

[9] M.E. Bianchi, M. Beltrame, G. Paonessa, Specific recognition of cruciform DNA by nuclear protein HMG1, Science 243 (4894 Pt 1) (1989) 1056–1059, https://doi.org/10.1126/science.2922595.

[10] S.A. Lee, M.S. Kwak, S. Kim, J.S. Shin, The role of high mobility group box 1 in innate immunity, Yonsei Med. J. 55 (5) (2014) 1165–1176, https://doi.org/10.3349/ymj.2014.55.5.1165.

[11] R.H. Blair, A.E. Horn, Y. Pazhani, L. Grado, J.A. Goodrich, J.F. Kugel, The HMGB1 C-terminal tail regulates DNA bending, J. Mol. Biol. 428 (20) (2016) 4060–4072, https://doi.org/10.1016/j.jmb.2016.08.018.

[12] L. Cato, K. Stott, M. Watson, J.O. Thomas, The interaction of HMGB1 and linker histones occurs through their acidic and basic tails, J. Mol. Biol. 384 (5) (2008) 1262–1272, https://doi.org/10.1016/j.jmb.2008.10.001.

[13] M.S. Kwak, W.J. Rhee, Y.J. Lee, H.S. Kim, Y.H. Kim, M.K. Kwon, J.S. Shin, Reactive oxygen species induce Cys106-mediated anti-parallel HMGB1 dimerization that protects against DNA damage, Redox Biol. 40 (2021) 101858, https://doi.org/10.1016/j.redox.2021.101858.

[14] H. Yanai, T. Ban, Z. Wang, M.K. Choi, T. Kawamura, H. Negishi, M. Nakasato, Y. Lu, S. Hangai, R. Koshiba, D. Savitsky, L. Ronfani, S. Akira, M.E. Bianchi, K. Honda, T. Tamura, T. Kodama, T. Taniguchi, HMGB proteins function as universal sentinels for nucleic-acid-mediated innate immune responses, Nature 462 (7269) (2009) 99–103, https://doi.org/10.1038/nature08512.

[15] M.T. Lotze, K.J. Tracey, High-mobility group box 1 protein (HMGB1): nuclear weapon in the immune arsenal, Nat. Rev. Immunol. 5 (4) (2005) 331–342, https://doi.org/10.1038/nri1594.

[16] J.H. Youn, J.S. Shin, Nucleocytoplasmic shuttling of HMGB1 is regulated by phosphorylation that redirects it toward secretion, J. Immunol. 177 (11) (2006) 7889–7897.

[17] Y.J. Oh, J.H. Youn, Y. Ji, S.E. Lee, K.J. Lim, J.E. Choi, J.S. Shin, HMGB1 is phosphorylated by classical protein kinase C and is secreted by a calcium-dependent mechanism, J. Immunol. 182 (9) (2009) 5800–5809, https://doi.org/10.4049/jimmunol.0801873.

[18] Y.J. Oh, J.H. Youn, H.J. Min, D.H. Kim, S.S. Lee, I.H. Choi, J.S. Shin, CKD712, (S)-1-(α-naphthylmethyl)-6,7-dihydroxy-1,2,3,4-tetrahydroisoquinoline, inhibits the lipopolysaccharide-stimulated secretion of HMGB1 by inhibiting PI3K and classical protein kinase C, Int. Immunopharm. 11 (9) (2011) 1160–1165, https://doi.org/10.1016/j.intimp.2011.03.013.

[19] S. Müller, P. Scaffidi, B. Degryse, T. Bonaldi, L. Ronfani, A. Agresti, M. Beltrame, M. E. Bianchi, The double life of HMGB1 chromatin protein: architectural factor and extracellular signal, EMBO J. 20 (16) (2001) 4337–4340, https://doi.org/10.1093/emboj/20.16.4337.

[20] H. Wang, O. Bloom, M. Zhang, J.M. Vishnubhakat, M. Ombrellino, J. Che, A. Frazier, H. Yang, S. Ivanova, L. Borovikova, K.R. Manogue, E. Faist, E. Abraham, J. Andersson, U. Andersson, P.E. Molina, N.N. Abumrad, A. Sama, K.J. Tracey, HMG-1 as a late mediator of endotoxin lethality in mice, Science 285 (5425) (1999) 248–251, https://doi.org/10.1126/science.285.5425.248.

[21] M.S. Kwak, H.S. Kim, B. Lee, Y.H. Kim, M. Son, J.S. Shin, Immunological significance of HMGB1 post-translational modification and redox biology, Front. Immunol. 11 (2020) 1189, https://doi.org/10.3389/fimmu.2020.01189.

[22] Y.H. Kim, M.S. Kwak, J.B. Park, S.A. Lee, J.E. Choi, H.S. Cho, J.S. Shin, N-linked glycosylation plays a crucial role in the secretion of HMGB1, J. Cell Sci. 129 (1) (2016) 29–38, https://doi.org/10.1242/jcs.176412.

[23] M.S. Kwak, H.S. Kim, K. Lkhamsuren, Y.H. Kim, M.G. Han, J.M. Shin, I.H. Park, W. J. Rhee, S.K. Lee, S.G. Rhee, J.S. Shin, Peroxiredoxin-mediated disulfide bond formation is required for nucleocytoplasmic translocation and secretion of HMGB1 in response to inflammatory stimuli, Redox Biol. 24 (2019) 101203, https://doi.org/10.1016/j.redox.2019.101203.

[24] Y.H. Kim, M.S. Kwak, B. Lee, J.M. Shin, S. Aum, I.H. Park, M.G. Lee, J.S. Shin, Secretory autophagy machinery and vesicular trafficking are involved in HMGB1 secretion, Autophagy 17 (9) (2021) 2345–2362, https://doi.org/10.1080/15548627.2020.1826690.

[25] J.H. Youn, Y.J. Oh, E.S. Kim, J.E. Choi, J.S. Shin, High mobility group box 1 protein binding to lipopolysaccharide facilitates transfer of lipopolysaccharide to CD14 and enhances lipopolysaccharide-mediated TNF-alpha production in human monocytes, J. Immunol. 180 (7) (2008) 5067–5074.

[26] J. Tian, A.M. Avalos, S.Y. Mao, B. Chen, K. Senthil, H. Wu, P. Parroche, S. Drabic, D. Golenbock, C. Sirois, J. Hua, L.L. An, L. Audoly, G. La Rosa, A. Bierhaus, P. Naworth, A. Marshak-Rothstein, M.K. Crow, K.A. Fitzgerald, E. Latz, P.A. Kiener, A.J. Coyle, Toll-like receptor 9-dependent activation by DNA-containing immune complexes is mediated by HMGB1 and RAGE, Nat. Immunol. 8 (5) (2007) 487–496, https://doi.org/10.1038/ni1457.

[27] H.J. Huttunen, C. Fages, H. Rauvala, Receptor for advanced glycation end products (RAGE)-mediated neurite outgrowth and activation of NF-kappaB require the cytoplasmic domain of the receptor but different downstream signaling pathways, J. Biol. Chem. 274 (28) (1999) 19919–19924, https://doi.org/10.1074/jbc.274.28.19919.

[28] S. Kim, S.Y. Kim, J.P. Pribis, M. Lotze, K.P. Mollen, R. Shapiro, P. Loughran, M. J. Scott, T.R. Billiar, Signaling of high mobility group box 1 (HMGB1) through toll-like receptor 4 in macrophages requires CD14, Mol. Med. 19 (1) (2013) 88–98, https://doi.org/10.2119/molmed.2012.00306.

[29] N.W. Schröder, S. Morath, C. Alexander, L. Hamann, T. Hartung, U. Zähringer, U. B. Göbel, J.R. Weber, R.R. Schumann, Lipoteichoic acid (LTA) of Streptococcus pneumoniae and Staphylococcus aureus activates immune cells via Toll-like receptor (TLR)-2, lipopolysaccharide-binding protein (LBP), and CD14, whereas TLR-4 and MD-2 are not involved, J. Biol. Chem. 278 (18) (2003) 15587–15594, https://doi.org/10.1074/jbc.M212829200.

[30] M.S. Kwak, M. Lim, Y.J. Lee, H.S. Lee, Y.H. Kim, J.H. Youn, J.E. Choi, J.S. Shin, HMGB1 binds to lipoteichoic acid and enhances TNF-α and IL-6 production through HMGB1-mediated transfer of lipoteichoic acid to CD14 and TLR2, J. Innate Immun. 7 (4) (2015) 405–416, https://doi.org/10.1159/000369972.

[31] Y. Sha, J. Zmijewski, Z. Xu, E. Abraham, HMGB1 develops enhanced proinflammatory activity by binding to cytokines, J. Immunol. 180 (4) (2008) 2531–2537, https://doi.org/10.4049/jimmunol.180.4.2531.

[32] J.H. Youn, M.S. Kwak, J. Wu, E.S. Kim, Y. Ji, H.J. Min, J.H. Yoo, J.E. Choi, H. S. Cho, J.S. Shin, Identification of lipopolysaccharide-binding peptide regions within HMGB1 and their effects on subclinical endotoxemia in a mouse model, Eur. J. Immunol. 41 (9) (2011) 2753–2762, https://doi.org/10.1002/eji.201141391.

[33] M.S. Jin, S.E. Kim, J.Y. Heo, M.E. Lee, H.M. Kim, S.G. Paik, H. Lee, J.O. Lee, Crystal structure of the TLR1-TLR2 heterodimer induced by binding of a tri-acylated lipopeptide, Cell 130 (6) (2007) 1071–1082, https://doi.org/10.1016/j.cell.2007.09.008.

[34] C.L. Krüger, M.T. Zeuner, G.S. Cottrell, D. Widera, M. Heilemann, Quantitative single-molecule imaging of TLR4 reveals ligand-specific receptor dimerization, Sci. Signal. 10 (503) (2017), https://doi.org/10.1126/scisignal.aan1308.

[35] A. Moysa, K. Steczkiewicz, D. Niedzialek, D. Hammerschmid, L. Zhukova, F. Sobott, M. Dadlez, A model of full-length RAGE in complex with S100B, Structure 29 (9) (2021) 989–1002, https://doi.org/10.1016/j.str.2021.04.002, e1006.

[36] T. Ostendorp, E. Leclerc, A. Galichet, M. Koch, N. Demling, B. Weigle, C. W. Heizmann, P.M. Kroneck, G. Fritz, Structural and functional insights into RAGE activation by multimeric S100B, EMBO J. 26 (16) (2007) 3868–3878, https://doi.org/10.1038/sj.emboj.7601805.

[37] S. Sun, M. He, S. VanPatten, Y. Al-Abed, Mechanistic insights into high mobility group box-1 (HMGb1)-induced Toll-like receptor 4 (TLR4) dimer formation, J. Biomol. Struct. Dyn. 37 (14) (2019) 3721–3730, https://doi.org/10.1080/07391102.2018.1526712.

[38] E. Thulin, T. Kesvatera, S. Linse, Molecular determinants of S100B oligomer formation, PLoS One 6 (3) (2011) e14768, https://doi.org/10.1371/journal.pone.0014768.

[39] A. Basset, F. Zhang, C. Benes, S. Sayeed, M. Herd, C. Thompson, D.T. Golenbock, A. Camilli, R. Malley, Toll-like receptor (TLR) 2 mediates inflammatory responses to oligomerized RrgA pneumococcal pilus type 1 protein, J. Biol. Chem. 288 (4) (2013) 2665–2675, https://doi.org/10.1074/jbc.M112.398875.

[40] W.L. Anggayasti, R.L. Mancera, S. Bottomley, E. Helmerhorst, The effect of physicochemical factors on the self-association of HMGB1: a surface plasmon resonance study, Biochim. Biophys. Acta 1864 (11) (2016) 1620–1629, https://doi.org/10.1016/j.bbapap.2016.07.008.

[41] W.L. Anggayasti, R.L. Mancera, S. Bottomley, E. Helmerhorst, Optimization of surface plasmon resonance experiments: case of high mobility group box 1 (HMGB1) interactions, Anal. Biochem. 499 (2016) 43–50, https://doi.org/10.1016/j.ab.2015.12.024.

[42] W.L. Anggayasti, R.L. Mancera, S. Bottomley, E. Helmerhorst, The self-association of HMGB1 and its possible role in the binding to DNA and cell membrane receptors, FEBS Lett. 591 (2) (2017) 282–294, https://doi.org/10.1002/1873-3468.12545.

[43] H. Yang, H.S. Hreggvidsdottir, K. Palmblad, H. Wang, M. Ochani, J. Li, B. Lu, S. Chavan, M. Rosas-Ballina, Y. Al-Abed, S. Akira, A. Bierhaus, H. Erlandsson-Harris, U. Andersson, K.J. Tracey, A critical cysteine is required for HMGB1 binding to Toll-like receptor 4 and activation of macrophage cytokine release, Proc. Natl. Acad. Sci. U. S. A. 107 (26) (2010) 11942–11947, https://doi.org/10.1073/pnas.1003893107.

[44] H. Kazama, J.E. Ricci, J.M. Herndon, G. Hoppe, D.R. Green, T.A. Ferguson, Induction of immunological tolerance by apoptotic cells requires caspase-dependent oxidation of high-mobility group box-1 protein, Immunity 29 (1) (2008) 21–32, https://doi.org/10.1016/j.immuni.2008.05.013.

[45] M. Schiraldi, A. Raucci, L.M. Munoz, E. Livoti, B. Celona, E. Venereau, T. Apuzzo, F. De Marchis, M. Pedotti, A. Bachi, M. Thelen, L. Varani, M. Mellado, A. Proudfoot, M.E. Bianchi, M. Uguccioni, HMGB1 promotes recruitment of inflammatory cells to damaged tissues by forming a complex with CXCL12 and signaling via CXCR4, J. Exp. Med. 209 (3) (2012) 551–563, https://doi.org/10.1084/jem.20111739.

[46] E. Venereau, M. Casalgrandi, M. Schiraldi, D.J. Antoine, A. Cattaneo, F. De Marchis, J. Liu, A. Antonelli, A. Preti, L. Raeli, S.S. Shams, H. Yang, L. Varani, U. Andersson, K.J. Tracey, A. Bachi, M. Uguccioni, M.E. Bianchi, Mutually exclusive redox forms of HMGB1 promote cell recruitment or proinflammatory cytokine release, J. Exp. Med. 209 (9) (2012) 1519–1528, https://doi.org/10.1084/jem.20120189.

[47] Y. Aida, M.J. Pabst, Removal of endotoxin from protein solutions by phase separation using Triton X-114, J. Immunol. Methods 132 (2) (1990) 191–195, https://doi.org/10.1016/0022-1759(90)90029-u.

[48] A. Jain, R. Liu, B. Ramani, E. Arauz, Y. Ishitsuka, K. Ragunathan, J. Park, J. Chen, Y.K. Xiang, T. Ha, Probing cellular protein complexes using single-molecule pull-down, Nature 473 (7348) (2011) 484–488, https://doi.org/10.1038/nature10016.

[49] H. Yang, P. Lundback, L. Ottosson, H. Erlandsson-Harris, E. Venereau, M. E. Bianchi, Y. Al-Abed, U. Andersson, K.J. Tracey, Redox modifications of cysteine residues regulate the cytokine activity of HMGB1, Mol. Med. 27 (1) (2021) 58, https://doi.org/10.1186/s10020-021-00307-1.

[50] A.E. Fazary, N.S. Awwad, H.A. Ibrahium, A.A. Shati, M.Y. Alfaifi, Y.H. Ju, Protonation equilibria of N-acetylcysteine, ACS Omega 5 (31) (2020) 19598–19605, https://doi.org/10.1021/acsomega.0c02080.
[51] B.S. Shah, K.G. Burt, T. Jacobsen, T.D. Fernandes, D.O. Alipui, K.T. Weber, M. Levine, S.S. Chavan, H. Yang, K.J. Tracey, N.O. Chahine, High mobility group box-1 induces pro-inflammatory signaling in human nucleus pulposus cells via toll-like receptor 4-dependent pathway, J. Orthop. Res. 37 (1) (2019) 220–231, https://doi.org/10.1002/jor.24154.
[52] S. Ivanov, A.M. Dragoi, X. Wang, C. Dallacosta, J. Louten, G. Musco, G. Sitia, G. S. Yap, Y. Wan, C.A. Biron, M.E. Bianchi, H. Wang, W.M. Chu, A novel role for HMGB1 in TLR9-mediated inflammatory responses to CpG-DNA, Blood 110 (6) (2007) 1970–1981, https://doi.org/10.1182/blood-2006-09-044776.
[53] M. Deng, Y. Tang, W. Li, X. Wang, R. Zhang, X. Zhang, X. Zhao, J. Liu, C. Tang, Z. Liu, Y. Huang, H. Peng, L. Xiao, D. Tang, M.J. Scott, Q. Wang, J. Liu, X. Xiao, S. Watkins, J. Li, H. Yang, H. Wang, F. Chen, K.J. Tracey, T.R. Billiar, B. Lu, The endotoxin delivery protein HMGB1 mediates caspase-11-dependent lethality in sepsis, Immunity 49 (4) (2018) 740–753, https://doi.org/10.1016/j.immuni.2018.08.016, e747.
[54] S. Saitoh, S. Akashi, T. Yamada, N. Tanimura, F. Matsumoto, K. Fukase, S. Kusumoto, A. Kosugi, K. Miyake, Ligand-dependent Toll-like receptor 4 (TLR4)-oligomerization is directly linked with TLR4-signaling, J. Endotoxin Res. 10 (4) (2004) 257–260, https://doi.org/10.1179/096805104225005904.
[55] A. Moysa, D. Hammerschmid, R.H. Szczepanowski, F. Sobott, M. Dadlez, Enhanced oligomerization of full-length RAGE by synergy of the interaction of its domains, Sci. Rep. 9 (1) (2019) 20332, https://doi.org/10.1038/s41598-019-56993-9.
[56] W. Abdulmahdi, D. Patel, M.M. Rabadi, T. Azar, E. Jules, M. Lipphardt, R. Hashemiyoon, B.B. Ratliff, HMGB1 redox during sepsis, Redox Biol. 13 (2017) 600–607, https://doi.org/10.1016/j.redox.2017.08.001.
[57] B.S. Park, D.H. Song, H.M. Kim, B.S. Choi, H. Lee, J.O. Lee, The structural basis of lipopolysaccharide recognition by the TLR4-MD-2 complex, Nature 458 (7242) (2009) 1191–1195, https://doi.org/10.1038/nature07830.
[58] M.S. Jin, J.O. Lee, Structures of the toll-like receptor family and its ligand complexes, Immunity 29 (2) (2008) 182–191, https://doi.org/10.1016/j.immuni.2008.07.007.
[59] H. Yang, H. Wang, Z. Ju, A.A. Ragab, P. Lundback, W. Long, S.I. Valdes-Ferrer, M. He, J.P. Pribis, J. Li, B. Lu, D. Gero, C. Szabo, D.J. Antoine, H.E. Harris, D. T. Golenbock, J. Meng, J. Roth, S.S. Chavan, U. Andersson, T.R. Billiar, K.J. Tracey, Y. Al-Abed, MD-2 is required for disulfide HMGB1-dependent TLR4 signaling, J. Exp. Med. 212 (1) (2015) 5–14, https://doi.org/10.1084/jem.20141318.